Journal of Solid Mechanics Vol. 6, No. 3 (2014) pp. 255-264

Investigation of Vibrational Behavior of Perfect and Defective Carbon Nanotubes Using Non–Linear Mass–Spring Model

A.A. Shariati , A.R. Golkarian , M. Jabbarzadeh*

Department of Mechanical Engineering, Mashhad Branch, Islamic Azad University, Mashhad, Iran

Received 28 March 2014; accepted 29 May 2014

ABSTRACT

In the present study, the effects of arrangement and distribution of multifarious types of defects on fundamental frequency of carbon nanotubes are investigated with respect to different chirality and boundary conditions. Interatomic interactions between each pair of carbon atoms are modeled using two types of non–linear spring–like elements. To obtain more information about the influences of defects; the effects of location, number and distribution (gathered or scattered defects) of two most common types of defects (vacancy and Stone–Wales defects) are examined on vibrational behavior of carbon nanotubes. Obtained results are in good agreement with the results reported in other literature. The results show that, gathered vacancy defects cause to a reduction in natural frequency of nanotubes, especially in the case of fix–fix boundary condition. It is also observed that the effect of defects depends on chirality intensively. In addition, the influence of the first vacancy defect is significantly more than the first Stone–Wales defect.

Keywords: Carbon nanotube; Vacancy defect; Stone–wales defect; Natural frequency; Non–linear spring

1 INTRODUCTION

CARBON nanotubes (CNTs) which are considered by many researchers because of their prominent physical and chemical properties, have been discovered in 1991 by Iijima [1]. Among the interesting mechanical [2-5], thermal [5-7], and electrical [8, 9] properties of CNTs, high elastic modulus, excellent tensile strength, remarkable thermal and electrical conductivity, significant strength to weight ratio and temperature stability up to 2800ºC in vacuum [5, 10, 11] could be mentioned. Abundant applications of CNTs in industry [12, 13], medicine [14] and engineering [15] are consequent of these exclusive characteristics.

Due to the high strength and low weight of CNTs, their vibrational frequencies are in order of GHz. In addition, abundant applications of this category of nano–materials such as producing nano–mechanical devices including oscillators, charge detectors, field emission devices and sensors [16], increase the necessity of investigation of their vibrational behavior. On another hand, the evaluation of effects of defects on properties of these nano–structures would be crucial because of the inevitable creation of defects during the synthesis and purification processes [17, 18] and under mechanical strains [19]. Among structural defects, vacancy and Stone–Wales (S–W) defects [20] are more prevalent and their numbers and locations would be unclear and it is necessary to investigate their influences from different points of view.

* Corresponding author. Tel.: +98 5116625046; Fax: +98 5116625046.
E-mail address: jabbarzadeh@mshdiau.ac.ir (M. Jabbarzadeh).

Indeed, several quests have been performed in order to understand the vibrational behavior of CNTs. Duan et al. [21] examined natural frequencies of armchair single walled carbon nanotubes (SWCNTs) by molecular dynamic (MD) method and commercial MD software MATERIALS–STUDIO and used obtained results to estimate the effects of aspect ratio, boundary conditions and mode shapes on small scaling parameter (e_0) in nonlocal Timoshenko beam theory. Hashemnia et al. [22] performed frequency analysis on SWCNTs and single layer graphene sheets (SLGSs) using beam element via MD method. Sakhaee–Pour et al. [23] offered simple and quick equation to predict natural frequencies according to geometric characteristics of SWCNTs (such as length and diameter). Also they evaluated natural frequencies and mode shapes of SWCNTs using 3D elastic beam element in finite element approach and regarded the influences of aspect ratio and boundary conditions. Georgantzinos and Anifantis [24] modeled multi walled carbon nanotubes (MWCNTs) using linear springs and point masses and solved an eigenvalue problem to gain natural frequencies and mode shapes of MWCNTs. In addition, they investigated the effects of aspect ratio, chirality and number of layers on natural frequency. Chowdhury et al. [25] studied natural frequencies of zigzag and armchair CNTs using molecular mechanics (MM) approach and found that natural frequency decreases when aspect ratio increases. Arghavan and Singh [26] analyzed free and forced vibration of SWCNTs and obtained natural frequencies and mode shapes by solving an eigenvalue problem. They considered different boundary conditions and observed that natural frequencies of armchair CNTs are lower than zigzag ones. Yan et al. [27] simulated CNTs using a space–frame model with flexible connections to determine fundamental frequencies with respect to different boundary conditions and aspect ratios. Joshi et al. [28] simulated CNTs by 3D elastic beam element and studied the efficacy of presence of vacancy defect on natural frequency for various size and chirality via finite element method. Also, the influence of number of defects was characterized and it was reported that by increasing the number of defects, natural frequency decreases. Parvaneh et al. [29] performed frequency analysis on zigzag SWCNTs using non–linear spring based model for different number of defects and boundary conditions. Ebrahim Zadeh et al. [30] used 3D elastic beam element to simulate CNTs and checked the effects of existence and position of vacancy defects on fundamental frequency. By assuming multifarious chirality and aspect ratio, it was observed that fundamental frequency decreases when aspect ratio and number of defects increase. Ansari et al. [31] investigated free vibration of SWCNTs and double walled carbon nanotubes (DWCNTs) using MD simulation. They considered different boundary conditions and dimensions and observed that by increasing the tube length, the natural frequency and its dependency on tube boundary condition is reduced. Ghavamian and Ochsner [32] studied vibrational behavior of CNTs with various numbers of layers using finite element method via MSC.Marc software. They evaluated the effects of three types of scattered defects (Si–doping, carbon vacancy and perturbation) and found that by increasing the number of scattered vacancy defects, frequency decreases.

In accomplished researches in this field, it is observed that usually MD method has been used to investigate vibrational behavior of CNTs, while in comparison with structural mechanics approach, it is an expensive method with high amount of computations and is applicable for limited scales. Also, in most of the researches which have been performed by FEM or structural mechanics approach, beam element has been used to simulate interatomic interactions while using beam or rod elements needs to define cross–section and inertia. In addition, the atomic mass of carbon atom which should be defined as point mass in the position of each carbon atom (node), has been assumed as the density of beam elements which causes errors especially for vibrational analysis (Fig. 1). On the other hand, the presence of defects in this category of nanostructures would be inevitable and investigating their mechanical behavior without taking it into account would be inappropriate.

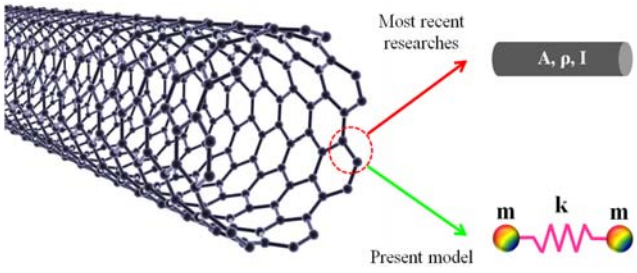

Fig. 1
Schematic view of replacing employed element to simulate CNTs by the present study.

In this paper, natural frequencies and mode shapes of armchair and zigzag SWCNTs with different boundary conditions using non–linear mass–spring model developed by Golkarian and Jabbarzadeh [33, 34] are investigated. Utilization of non–linear mass–spring model leads to prevent from above problems and increases the accuracy of calculations. In addition, a comprehensive investigation is performed on the influence of vacancy and S–W defects (as two common types of defects) on the vibrational frequency of SWCNTs. For this purpose, the effects of number of defects, their distribution or centralization and defects location are investigated. The employed CNTs are zigzag (11, 0) and armchair (7, 7) nanotubes, with length to radius ratio higher than 10 [35]. Vibrational analyses on more than 130 fully non–linear models are performed via finite element ABAQUS software and obtained results are compared with the results of other studies.

2 MODELING

CNTs are the result of arranging carbon atoms in a regular lattice with hexagonal cells (Fig. 2). In this structure, each carbon atom with three nearest carbon atoms constitutes covalent bonds. Based on molecular mechanics theory, summation of bonded and non–bonded energies which lead to produce force field between carbon atoms can be explained by potential energy functions with following equation [36]:

$$V = V_r + V_\theta + V_\varphi + V_\omega + V_{vdW} \tag{1}$$

where V_r represents the bond stretching energy, V_θ the bond angle bending energy, V_φ the dihedral angle torsion energy, V_ω the out–of–plane torsion energy and V_{vdW} the non–bonded energies of van der Waals interactions (Fig. 3). In Eq. (1) most portion of energies are associated with bond stretching energy and bond angle bending energy and the effects of other energies would be negligible [37].

Using Morse potential energy function [38], bond stretching energy can be stated by the following equation:

$$V_r = D_e\{[1-e^{-\beta(r-r_0)}]^2 - 1\} \tag{2}$$

where D_e=6.03105×10^{-10}, β=26.26 nm^{-1}, r_0=0.1421 nm and r is the current distance between two atoms. In addition, Morse potential offers following equation to obtain the bond angle bending energy:

$$V_\theta = \frac{1}{2}k_\theta(\Delta\theta)^2[1 + k_{sextic}(\Delta\theta)^4] \tag{3}$$

where k_θ=0.9×10^{-18} Nm/rad^2, $\Delta\theta$=θ–θ$_0$, θ_0=2.094 rad and k_{sextic}=0.754 rad^{-4}.

As illustrated in Fig. 2, in the present model, two kinds of non–linear translational springs "A" and "B" are used to simulate bond stretching and bond angle bending, respectively. In order to define these two kinds of springs, it is necessary to determine their force–displacement behavior. Based on the proven principles of mechanics, the force–displacement equation is derived from the first derivation of energy equation. Therefore the force–displacement behavior of springs group "A" which is used to simulate C–C bonds, derived from the first derivation of Eq. (2):

$$F(\Delta r) = 2\beta D_e(1-e^{-\beta\Delta r})e^{-\beta\Delta r} \tag{4}$$

where Δr is the deviation of bond length from its equilibrium distance (r_0). If instead of non–linear translational springs group "B", the non–linear torsional springs are used; their torque–angle deviation equation is derived from the first derivation of Eq. (3). But for more simplification, springs group "B" are assumed as translational springs. Therefore, their lengths variation (for small deformations) are related to the angles variation by the following equation [39]:

$$\Delta\theta = \frac{2\Delta R}{r_0} \tag{5}$$

where ΔR is the length variation of springs group "B" from its equilibrium distance. With substituting Eq. (5) in Eq. (3) and obtaining first derivation of Eq. (3), the force–displacement behavior of non–linear translational springs group "B" which is used to simulate interatomic interaction of two opposite carbon atoms in C–C–C bonds (Fig. 2) is derived:

$$F(\Delta R) = \frac{4}{r_0^2} k_\theta \Delta R[1 + \frac{48}{r_0^4} k_{sextic} (\Delta R)^4] \quad (6)$$

Force–displacement behavior of non–linear translational spring's group "A" and "B" (Eq. (4) and Eq. (6)) are illustrated in Fig. 4.

By description of behavior of spring–like elements, their dimension, coordinate systems, location of each carbon atom and the overall geometry of the models are programed in MATLAB software. Then, the geometry of the models as an output file is imported into the ABAQUS software. In ABAQUS software, boundary conditions, the mass of carbon atoms and the method of problem solving are determined and frequency analyses of the models are performed. Point masses equal to atomic mass of carbon atom (m_C=1.9943*10^{-26} kg) are attached to each node as carbon atoms. Analysis are performed in finite element ABAQUS 6.10 software and connector elements CONN3D2 are used to define non–linear springs. In order to create any kind of defects, necessary changes are employed into the initial geometry files.

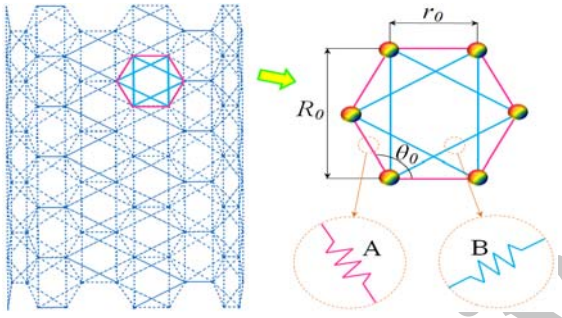

Fig. 2
Finite element model of CNT.

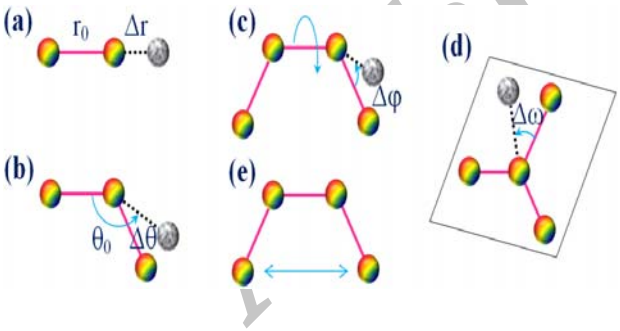

Fig. 3
Schematic view of bonded and non–bonded energies in molecular mechanics theory: a) stretching, b) angle bending, c) dihedral angle torsion, d) out–of–plane torsion and e) van der Waals interactions.

3 DEFECTS DESCRIPTION

The effects of two categories of defects are investigated in the present study: vacancy and S–W defects. Vacancy defects are created by missing one or more carbon atoms from the hexagonal lattice. To simulate each vacancy defect, that's enough to eliminate one carbon atom (node) and subsequently three corresponding spring elements from group "A" and six spring elements from group "B" (Fig. 5(a)) from lattice structure.

As it was mentioned, CNTs are a regular lattice with hexagonal cells but, as it is depicted in Fig. 5(b), sometimes due to the 90º rotation of C–C bonds, four hexagons which are associated with this bond, change to a pair of pentagon–pentagon and heptagon–heptagon cells which calls S–W defect. As it is obvious in Fig. 5(b), along with rotation of C–C bond, the length of C–C bonds remains constant in comparison with equilibrium distance (a_{C-C}), but angles deviate from their equilibrium status (θ_0) and consequently those springs which have been defined for

simulating the variations of these angles, will contain an initial tension or compression before applying any load or vibration. As a sample, when there is no S–W defect, if any load or vibration is applied on nanotube and leads to increase the size of an angle, the size of corresponding spring is also increased from its equilibrium point (point c in Fig. 4(b)) to a point like d. Now if due to presence of S–W defect, this spring contains an initial tension, its equilibrium point is depicted by point e (instead of point c) and by applying same load or vibration to the previous situation, point f will explain the status of mentioned spring. It's clear that due to the non–linearity of springs group "B", their force–displacement behavior are different for perfect and defective situation (part c–d and e–f in Fig. 4(b)) and these differences are considered in the present model by defining four stretched and compressed springs which are illustrated in Fig. 5(b).

In this paper, the effects of vacancy and S–W defects on the natural frequencies of zigzag and armchair CNTs are investigated from two different points of view by considering different boundary conditions. At first, the influence of position of one defect is examined. For this purpose, for free–fix boundary condition a vacancy defect moves along five different locations (Fig. 6) and the effect of this movement on the natural frequency is obtained. In addition, for fix–fix boundary condition, according to the symmetry of CNTs, locations 1 to 3 are investigated as illustrated in Fig. 6. In the second stage, the effect of increase in the number of defects and distribution of the defects (gathered or scattered defect) are explored. For this purpose, as is depicted in Fig. 7, initially one defect is created in location 1 and after that second to sixth defects added to their related positions, respectively and thereby the efficacy of increase in the number of defects from 1 to 6 defects on the natural frequency is evaluated, assuming all defects are concentrated in the center of the CNT. Then the same process is repeated when the defects are widely and randomly scattered in different locations of the CNT (Fig. 8). It should be noticed that the influence of S–W defects is checked in the same way. All the figures are schematically and related to the armchair CNTs and in the case of zigzag ones, each case would be same.

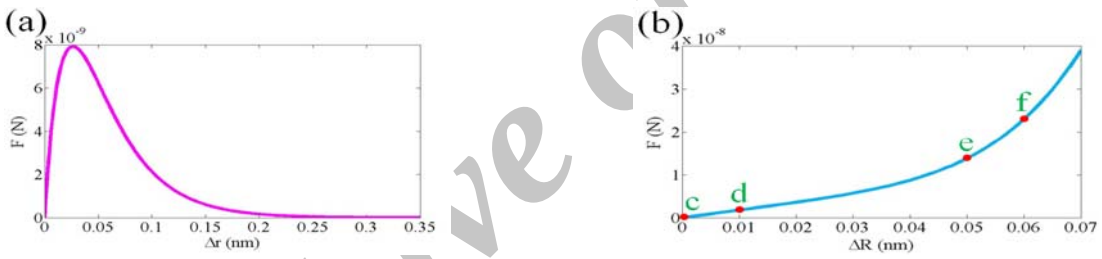

Fig. 4
Force–displacement behavior of non–linear spring's group a) "A" and b) "B".

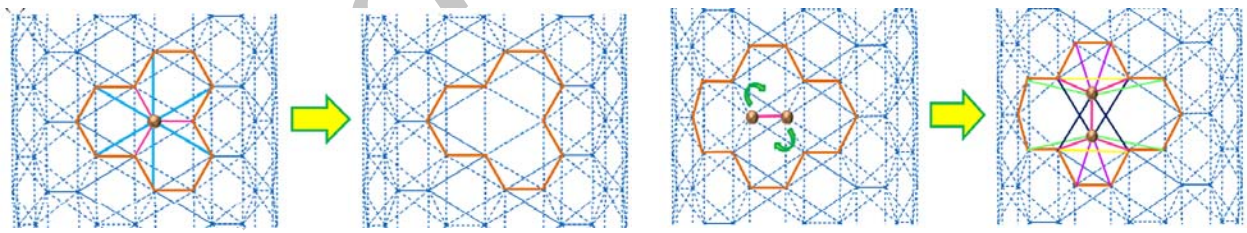

(a) (b)

Fig. 5
Introducing a) vacancy defect and b) S–W defect.

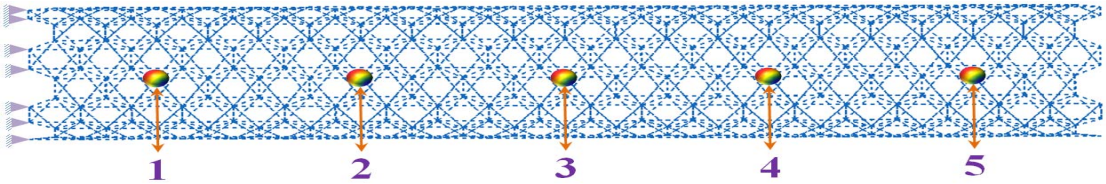

Fig.6
Selected locations of the defects.

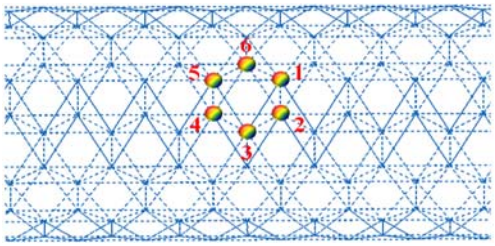

Fig. 7
The order of introducing six gathered defects in the center of CNT.

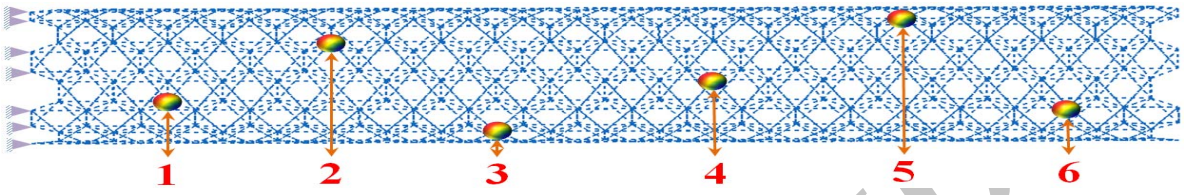

Fig. 8
The order of introducing six scattered defects in the CNT.

4 NUMERICAL RESULTS AND DISCUSSION

In order to validate the present method, at first natural frequencies of perfect CNTs for various dimensions and boundary conditions are obtained and compared with the results of other researches. Then the study in the case of defective CNTs is continued. Table 1 shows agreement of obtained results with other references.

In the present study two types of nanotubes with the same numbers of carbon atoms and different chiralities are used to investigate the effects of defects and their geometry, aspect ratio and fundamental frequency are shown in Table 2. As a sample, for fix–fix boundary condition, first mode shape of defective zigzag CNTs with six numbers of vacancy and S–W defects are illustrated in Figs. 9 and 10, respectively. Table 3. and Table 4. present obtained results related to the influence of location of one defect with respect to the chirality, defect type and boundary conditions and demonstrate that, CNTs with different chirality have completely different behavior. As it can be seen, for free–fix boundary condition, by increasing the distance between the location of vacancy defect and support, natural frequency of defective armchair CNT decreases while natural frequency of defective zigzag CNT increases. Almost the same trends is observed in the case of S–W defect with fix–fix boundary condition. In the case of free–fix boundary condition, vacancy and S–W defects have totally different effect on the natural frequency of armchair CNTs. From the results, it could be deduced that vacancy defects are more effective than S–W defects and extent of this effect depends on chirality, intensively.

Table 1
Presenting fundamental frequency of perfect CNTs in order to validate the model

Type of CNT	Aspect ratio	Boundary condition	Fundamental frequency (GHz) [21]	Fundamental frequency (GHz) [22]	Fundamental frequency (GHz) [25]	Fundamental frequency (GHz) [27]	Fundamental frequency (GHz) [31]	Fundamental frequency (GHz) Present model
(5,5)	5.44	Free–fix	200	–	207.5	–	208	222
(5,5)	5.44	Fix–fix	–	–	–	620	–	681
(6,6)	5.44	Free–fix	–	160	–	–	–	187

Table 2
Properties of employed CNTs

Type of CNT	Dimensions (nm)		Aspect ratio	Fundamental frequency for free–fix B.C. (GHz)	Fundamental frequency for fix–fix B.C. (GHz)
	Diameter	Length			
(7,7)	0.9499	5.1686	5.44	143.472	373.148
(11,0)	0.8618	4.7603	5.52	168.659	534.727

Table 3
The variation of fundamental frequency versus the defect location for free–fix boundary condition

Defect's location	Armchair natural frequency (GHz)		Zigzag natural frequency (GHz)	
	Vacancy defect	S–W defect	Vacancy defect	S–W defect
1	143.247	143.377	165.275	168.878
2	143.365	143.418	166.947	168.718
3	143.278	143.572	168.099	168.640
4	142.807	144.200	168.732	168.594
5	141.485	145.197	169.036	168.629

Table 4
The variation of fundamental frequency versus the defect location for fix–fix boundary condition

Defect's location	Armchair natural frequency (GHz)		Zigzag natural frequency (GHz)	
	Vacancy defect	S–W defect	Vacancy defect	S–W defect
1	372.085	373.464	533.951	533.854
2	372.143	373.550	529.987	531.178
3	370.558	373.719	526.600	529.856

The variations of frequency versus number of defects for free–fix boundary condition are illustrated in Figs. 11 and 12. In comparison with perfect CNT, by increasing the number of vacancy defects, natural frequency decreases for both chiralities and especially due to existence of six numbers of gathered vacancy defects, natural frequency of zigzag CNT decreases about 23 GHz. Although in the case of S–W defects, by increasing the number of defects, frequency increases for both chiralities and particularly due to presence of six numbers of scattered S–W defects, natural frequency of armchair CNT increases about 13 GHz. Also, unlike to armchair CNT, vacancy defects are more effective than S–W defects in zigzag one. Consequently it should be noticed that in this case, chirality is an important factor in determining the effects of defects on natural frequency, too.

In the case of fix–fix boundary condition, the influences of number of different defects on natural frequency are depicted in Figs. 13 and 14. Vacancy defect leads to a reduction in frequency for both chiralities, while S–W defects leads to increase in the frequency of armchair CNTs and a reduction in the case of zigzag ones. Also, for both zigzag and armchair CNTs, effect of vacancy defects would be more significant than S–W defects. Gathered vacancy defect, leads to decrease about 86 GHz in natural frequency of zigzag CNT for six numbers of defects. As a consequent, it could be stated that the effects of scattered vacancy and S–W defects on natural frequency of zigzag CNT almost are the same and in the case of armchair CNT the effect of distributed vacancy defects is negligible.

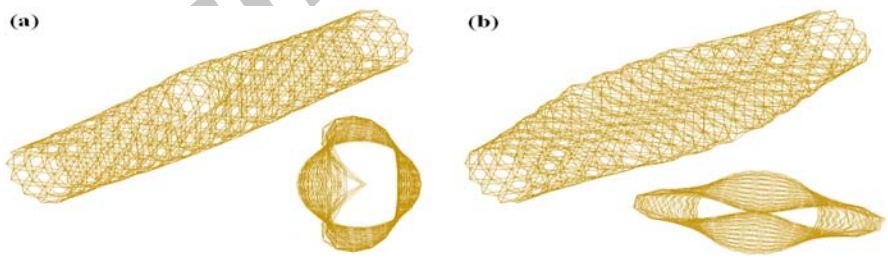

Fig.9
First mode shapes of defective zigzag CNT with six numbers of a) gathered and b) scattered vacancy defects.

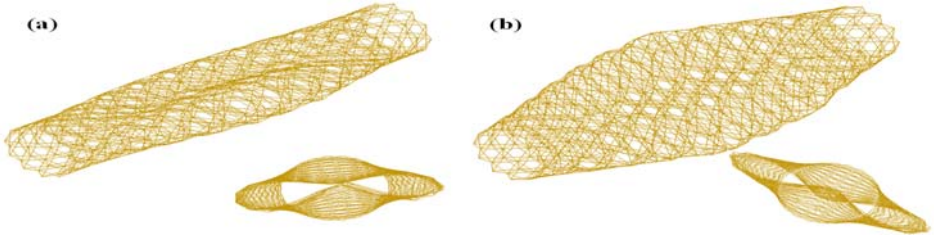

Fig.10
First mode shapes of defective zigzag CNT with six numbers of a) gathered and b) scattered S–W defects.

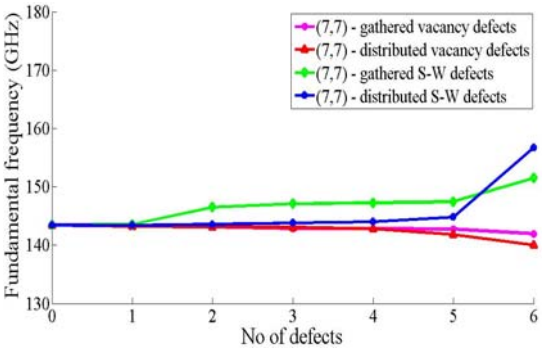

Fig. 11
Fundamental frequency of armchair CNT versus the number of defects for free–fix boundary condition.

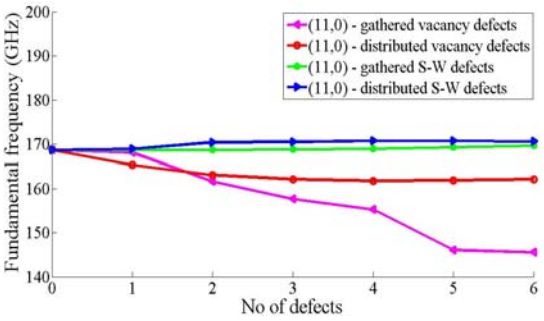

Fig. 12
Fundamental frequency of zigzag CNT versus the number of defects for free–fix boundary condition.

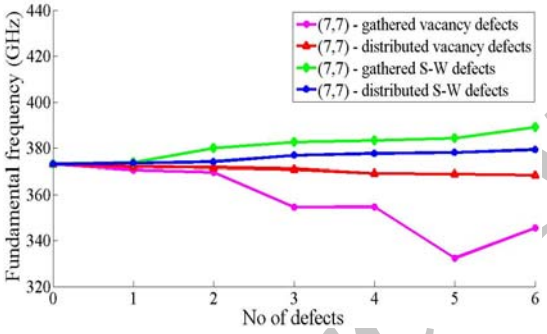

Fig. 13
Fundamental frequency of armchair CNT versus the number of defects for fix–fix boundary condition.

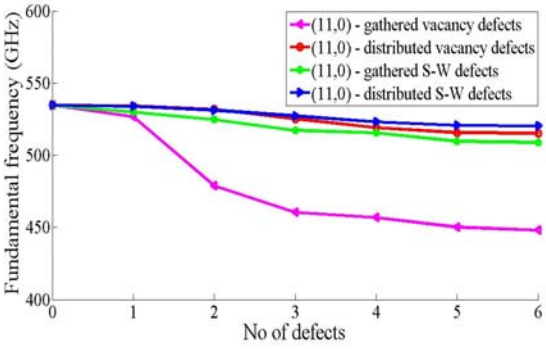

Fig. 14
Fundamental frequency of zigzag CNT versus the number of defects for fix–fix boundary condition.

5 CONCLUSIONS

In the present study CNTs are simulated using non–linear mass–spring model. Also the effects of location, number and arrangement of vacancy and S–W defects on natural frequency of CNTs are examined with respect to chirality and boundary conditions. The most important obtained results are:

- Natural frequency of perfect and defective zigzag CNTs are higher than armchair ones.
- For both zigzag and armchair CNTs, natural frequency of fix–fix boundary condition is higher than free–fix state.
- The effect of defects on the natural frequency depends on chirality and boundary conditions intensively.
- For one defect, vacancy defect is more effective than S–W defect on the natural frequency of CNTs.
- For free–fix boundary condition, by increasing the number of vacancy defects, frequency decreases while presence of S–W defects leads to an increase in frequency.
- Due to presence of gathered vacancy defects, natural frequency of zigzag CNTs reduced.
- In the case of fix–fix boundary condition, a few number of distributed vacancy defects have a negligible effect on natural frequency of armchair CNTs.

REFERENCES

[1] Iijima S., 1991, Helical microtubules of graphitic carbon, *Nature* **354**: 56-58.

[2] Demczyk B.G., Wang Y.M., Cumings J., Hetman M., Han W., Zettl A., 2002, Direct mechanical measurement of the tensile strength and elastic modulus of multiwalled carbon nanotubes, *Materials Science and Engineering A* **334**: 173-178.

[3] Goze C., Vaccarini L., Henrard L., Bernier P., Hernandez E., Rubio A., 1999, Elastic and mechanical properties of carbon nanotubes, *Synthetic Metals* **103**: 2500-2501.

[4] Krishnan A., Dujardin E., Ebbesen T.W., Yianilos P.N., Treacy M.M.J., 1998, Young's modulus of single–walled nanotubes, *Physical Review B* **58**(20): 14013-14019.

[5] Popov V.N., 2004, Carbon nanotubes: properties and applications, *Materials Science and Engineering R* **43**: 61-102.

[6] Ruoff R.S., Lorents D.C., 1995, Mechanical and thermal properties of carbon nanotubes, *Carbon* **33**: 925-930.

[7] Lasjaunias J. C., 2003, Thermal properties of carbon nanotubes, *C R Physique* **4**: 1047-1054.

[8] Issi J.P., Langer L., Heremans J., Olk C.H., 1995, Electronic properties of carbon nanotubes: experimental results, *Carbon* **33**: 941-948.

[9] Mintmire J.W., White C.T., 1995, Electronic and structural properties of carbon nanotubes, *Carbon* **33**: 893-902.

[10] Thostenson E.T., Ren Z., Chou T.W., 2001, Advanced in the science and technology of carbon nanotubes and their composites: a review, *Composite Science and Technology* **61**: 1899-1912.

[11] Ruoff R.S., Qian D., Liu W.K., 2003, Mechanical properties of carbon nanotubes: theoretical predictions and experimental measurements, *C R Physique* **4**: 993-1008.

[12] Paradise M., Goswami T., 2007, Carbon nanotubes production and industrial applications, *Materials and Design* **28**: 1477-1489.

[13] Hoenlein W., Kreupl F., Duesberg G.S., Graham A.P., Liebau M., Seidel R., 2003, Carbon nanotubes for microelectronics: status and future prospects, *Materials Science and Engineering C* **23**: 663-669.

[14] Tran P.A., Zhang L., Webster T.J., 2009, Carbon nanofibers and carbon nanotubes in regenerative medicine, *Advanced Drug Delivery Reviews* **61**: 1097-1114.

[15] Li C., Thostenson E.T., Chou T.W., 2008, Sensors and actuators based on carbon nanotubes and their composites: A review, *Composites Science and Technology* **68**: 1227-1249.

[16] Gibson R.F., Ayorinde E.O., Wen Y.F., 2007, Vibrations of carbon nanotubes and their composites: A review, *Composites Science and Technology* **67**: 1-28.

[17] Andrews R., Jacques D., Qian D., Dickey E.C., 2001, Purification and structural annealing of multiwalled carbon nanotubes at graphitization temperatures, *Carbon* **39**: 1681-1687.

[18] Mawhinney D.B., Naumenko V., Kuznetsova A., Yates Jr. J.T., Liu J., Smalley R.E., 2000, Surface defect site density on single walled carbon nanotubes by titration, *Chemical Physics Letters* **324**: 213-216.

[19] Nardelli M.B., Fattebert J.L., Orlikowski D., Roland C., Zhao Q., Bernholc J., 2000, Mechanical properties, defects and electronic behavior of carbon nanotubes, *Carbon* **38**: 1703-1711.

[20] Terrones M., Botello–Mendez A.R., Campos-Delgado J., Lopez-Urias F., Vega-Cantu Y.I., Rodriguez-Macias F.J., 2010, Graphene and graphite nanoribbons: Morphology, properties, synthesis, defects and applications, *Nano Today* **5**: 351-372.

[21] Duan W.H., Wang C.M., Zhang Y.Y., 2007, Calibration of nonlocal scaling effect parameter for free vibration of carbon nanotubes by molecular dynamics, *Journal of Applied Physics* **101**: 024305.

[22] Hashemnia K., Farid M., Vatankhah R., 2009, Vibrational analysis of carbon nanotubes and graphene sheets using molecular structural mechanics approach, *Computational Materials Science* **47**: 79-85.

[23] Sakhaee–Pour A., Ahmadian M.T., Vafai A., 2009, Vibrational analysis of single–walled carbon nanotubes using beam element, *Thin–Walled Structures* **47**: 646-652.

[24] Georgantzinos S.K., Anifantis N.K., 2009, Vibration analysis of multi–walled carbon nanotubes using a mass–spring based finite element model, *Computational Materials Science* **47**: 168-177.

[25] Chowdhury R., Adhikari S., Wang C.Y., Scarpa F., 2010, A molecular mechanics approach for the vibration of single–walled carbon nanotubes, *Computational Materials Science* **48**: 730-735.
[26] Arghavan S., Singh A.V., 2011, On the vibrations of single–walled carbon nanotubes, *Journal of Sound and Vibration* **330**: 3102-3122.
[27] Yan Y., Shi G., Zhao P., 2011, Frequency study of single–walled carbon nanotubes based on a space–frame model with flexible connections, *Journal of Computers* **6**: 1125-1130.
[28] Joshi A.Y., Sharma S.C., Harsha S.P., 2011, The effect of pinhole defect on vibrational characteristics of single walled carbon nanotube, *Physica E* **43**: 1040-1045.
[29] Parvaneh V., Shariati M., Torabi H., 2011, Frequency analysis of perfect and defective SWCNTs, *Computational Materials Science* **50**: 2051-2056.
[30] Ebrahim Zadeh Z., Yadollahpour M., Ziaei-Rad S., Karimzadeh F., 2012, The effect of vacancy defects and temperature on fundamental frequency of single walled carbon nanotubes, *Computational Materials Science* **63**: 12-19.
[31] Ansari R., Ajori S., Arash B., 2012, Vibrations of single- and double-walled carbon nanotubes with layerwise boundary conditions: A molecular dynamics study, *Current Applied Physics* **12**: 707-711.
[32] Ghavamian A., Ochsner A., 2013, Numerical modeling of eigen modes and eigenfrequencies of single- and multi-walled carbon nanotubes under the influence of atomic defects, *Computational Materials Science* **72**: 42-48.
[33] Golkarian A.R., Jabbarzadeh M., 2013, The density effect of van der Waals forces on the elastic modules in graphite layers, *Computational Materials Science* **74**: 138-142.
[34] Golkarian A.R., Jabbarzadeh M., 2012, The attitude of variation of elastic modules in single wall carbon nanotubes: nonlinear mass-spring model, *Journal of Solid Mechanics* **4**(1): 106-113.
[35] WenXing B., ChangChun Z., WanZhao C., 2004, Simulation of Young's modulus of single–walled carbon nanotubes by molecular dynamics, *Physica B* **352**: 156-163.
[36] Rappe A.K., Casewit C.J., Colwell K.S., Goddard W.A., Skiff W.M., 1992, A full periodic table force field for molecular mechanics and molecular dynamics simulations, *Journal of American Chemical Society* **114**: 10024-10035.
[37] Xiao J.R., Gama B.A., Gillespie Jr. J.W., 2005, An analytical molecular structural mechanics model for the mechanical properties of carbon nanotubes, *International Journal of Solids and Structures* **42**: 3075-3092.
[38] Machida K., 1999, *Principles of Molecular Structural Mechanics*,Wiley and Kodansha.
[39] Odegard G.M., Gates T.S., Nicholson L.M., Wise K.E., 2002, Equivalent–continuum modeling of nano–structured materials, *Composite Science and Technology* **62**: 1869-1880.